

# HTS Multi-Mode Ring Resonator UWB Filter with Cross-Shaped Stepped-Impedance Stubs

Zhihe Long<sup>1</sup>, Mingen Tian<sup>1</sup>, Liguang Zhou<sup>1</sup>, Shuangshuang Cao<sup>2</sup>,  
Man Qiao<sup>1</sup>, and Tianliang Zhang<sup>1,\*</sup>

**Abstract**—This paper presents an ultra-wideband (UWB) high temperature superconducting (HTS) bandpass filter (BPF) based on a ring resonator loaded with a pair of symmetrical cross-shaped stepped-impedance open stubs. The main advantages are that two transmission zeros are introduced to improve passband selectivity, and high mode suppression is achieved by adjusting the impedance ratio of the cross-shaped stubs and using a pair of parallel-coupled lines. The filter is designed on double-sided YBCO/MgO/YBCO HTS films with a thickness of 0.5 mm and dielectric constant of 9.8. At 77 K, the measured 3-dB bandwidth of the filter covers 1.63 GHz ~ 6.03 GHz. Due to the use of superconducting material, the insertion loss at the center frequency of 3.83 GHz is 0.12 dB, and the rejection is greater than 36 dB in the lower stopband, and the upper stopband with 20 dB attenuation level is extended to at least 8.5 GHz.

## 1. INTRODUCTION

The insertion loss and passband selectivity of conventional ultra-wideband (UWB) filters cannot satisfy the actual requirements on some occasions where high sensitivity and excellent anti-interference ability are required, mainly due to low Q value and high loss of the filter structure and the ordinary materials. Up till now researchers have done a lot of work on UWB filters to pursue these two significant characteristics. For example, the stub-loaded multi-mode resonator (SLMMR) and stepped impedance resonator (SIR) are often applied in the design of UWB filters due to their simple structures [1–3]. Various ring resonator UWB filters are also popularized because of many advantages of ring resonator such as compact size, high Q value and low loss [4–6].

In this paper, a new design of high temperature superconducting (HTS) UWB bandpass filter (BPF) is also advanced based on the ring resonator. A quintuple-mode ring resonator structure for realizing this HTS UWB filter with excellent out-of-band rejection and low insertion loss is provided. The advantages of this design are that the constructed ring resonator loaded with a pair of cross-shaped stepped-impedance stubs can generate five modes within the passband to easily satisfy the UWB requirement and a pair of transmission zeros near the passband to improve the selectivity. Also, by adjusting the impedance ratio of the cross-shaped stepped-impedance stubs and adding the appropriate external coupling strength through adopting the parallel-coupled lines, a high mode suppression is achieved, which means that a wider upper stopband is presented. Besides, because the UWB filter circuit was finally fabricated on the HTS thin films, extremely low insertion loss is realized, which is very attractive in the application of UWB communication system.

---

*Received 6 July 2018, Accepted 7 September 2018, Scheduled 23 September 2018*

\* Corresponding author: Tianliang Zhang (ztl@uestc.edu.cn).

<sup>1</sup> School of Aeronautics and Astronautics, University of Electronic Science and Technology of China, Chengdu 611731, China. <sup>2</sup> Dezhou University, Dezhou 253023, China.

## 2. DESIGN OF PROPOSED HTS UWB BPF

Figure 1(a) shows the proposed resonator. Due to its symmetrical structure, odd and even mode analytical method is applied to analyze it.

For the odd-mode case, the odd-mode circuit structure is shown in Figure 1(b). By using the odd and even mode analytical method and transmission line theory, the equivalent input impedance can be obtained through Equation (1).

$$Z_{in-odd} = jZ_1 \frac{2Z_1 \tan \theta_1 + Z_2 \tan \theta_2}{2Z_1 - Z_2 \tan \theta_1 \tan \theta_2} \quad (1)$$

$$\tan \theta_1 \tan \theta_2 = 2Z_1/Z_2 \quad (2)$$

Under the odd-mode resonant condition,  $Z_{in-odd}$  is equal to infinity, which derives Equation (2). It can be seen that only the impedance ratio  $Z_1/Z_2$  and the electric lengths  $\theta_1, \theta_2$  can affect the odd-mode resonant frequencies.

For the even-mode case, the even-mode circuit structure is shown in Figure 1(c). And the equivalent input impedance of even-mode circuit can be derived from Equations (3)–(7).

$$Z_a = jZ_4 \frac{Z_5^2 \tan \theta_4 \tan \theta_5 - Z_4 Z_5 + Z_4 Z_5 \tan^2 \theta_4 + Z_4^2 \tan \theta_4 \tan \theta_5}{2Z_4 Z_5 \tan \theta_4 + Z_4^2 \tan \theta_5 - Z_5^2 \tan^2 \theta_4 \tan \theta_5} \quad (3)$$

$$Z_L = \frac{1}{2} Z_{in-crossing} = Z_3 \frac{Z_a + jZ_3 \tan \theta_3}{2(Z_3 + jZ_a \tan \theta_3)} \quad (4)$$

$$Z_{up} = Z_2 \frac{Z_L + jZ_2 \tan \theta_2}{Z_2 + jZ_L \tan \theta_2} \quad (5)$$

$$Z_{down} = \frac{Z_2}{j \tan \theta_2} \quad (6)$$

$$Z_{in-even} = Z_1 \frac{Z_{up} Z_{down} + jZ_1 (Z_{up} + Z_{down}) \tan \theta_1}{Z_1 (Z_{up} + Z_{down}) + jZ_{up} Z_{down} \tan \theta_1} \quad (7)$$

$$Z_1 (Z_{up} + Z_{down}) + jZ_{up} Z_{down} \tan \theta_1 = 0 \quad (8)$$

Under the even-mode resonant condition,  $Z_{in-even}$  is equal to infinity, which obtains Equation (8). It can be known that besides  $Z_1/Z_2, \theta_1, \theta_2$ , the characteristic impedances and electric lengths of each part of the symmetrical cross-shaped stepped-impedance open stubs also determine the even-mode resonant frequencies. Therefore, by adjusting these parameters, the controllable odd-mode and even-mode resonant frequencies can distribute in the passband relatively equidistant to each other to form the UWB band.

As shown in Figure 2, the proposed UWB BPF consists of a quintuple-mode resonator mentioned above and a pair of parallel-coupled lines with stepped-impedance ports, whose slot width and line width can be changed to satisfy the external coupling strength.

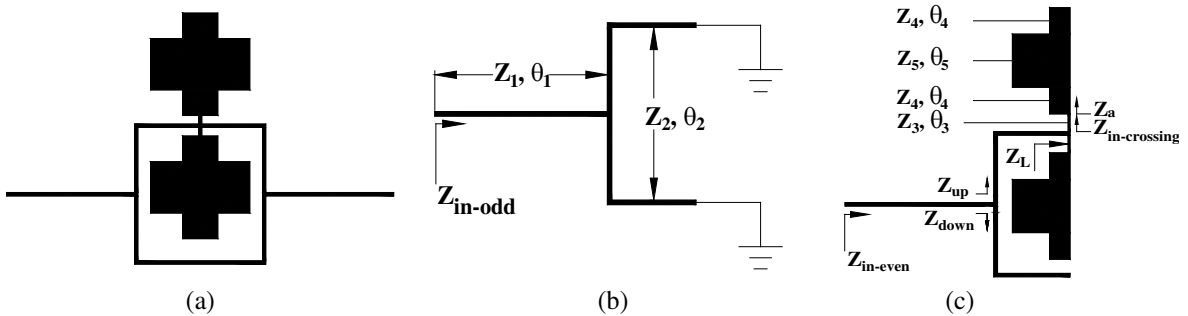


**Figure 1.** Analysis of odd and even modes. (a) The proposed resonator, (b) odd-mode circuit, (c) even-mode circuit.

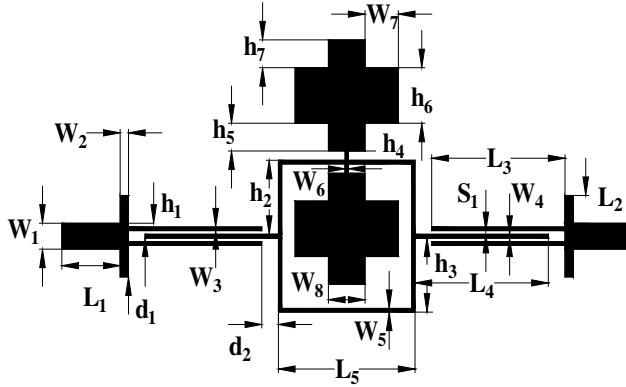


**Figure 2.** Schematic of the HTS ring resonator UWB filter.

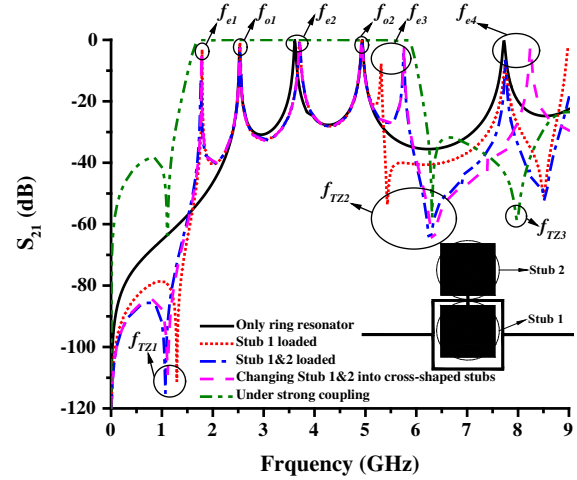


**Figure 3.** Analysis of the stubs with different shapes under weak/strong external coupling.

The function of this pair of cross-shaped stepped-impedance open stubs can be analyzed in the situation of weak-coupling feed. As shown in Figure 3, the square ring resonator without any loaded stubs is a triple-mode resonator. When a common stepped-impedance open stub (Stub 1) is loaded in the center upside position of this ring resonator, two new even modes ( $f_{e1}$  and  $f_{e3}$ ) and a pair of transmission zeros ( $f_{TZ1}$  and  $f_{TZ2}$ ) are generated simultaneously. As studied in [2], stepped-impedance open stub in resonator could introduce transmission zeros to achieve sharp passband selectivity. It can be seen that  $f_{e1}$  and  $f_{TZ1}$  are located in the low frequency, while  $f_{e3}$  and  $f_{TZ2}$  are situated in the high frequency range. Due to the introduction of these two transmission zeros, the passband selectivity is effectively improved. But the distance between  $f_{o2}$  and  $f_{e3}$  is relatively near, and at the same time, an unwanted high mode ( $f_{e4}$ ) is also produced which has a serious impact on the performance of upper stopband. Subsequently, another identical normal stepped-impedance open stub (Stub 2) is added out of the ring resonator, which leads to the further separation of  $f_{o2}$  and  $f_{e3}$ . Then changing the two ordinary stepped-impedance open stubs (Stub 1&2) into cross-shaped ones, it can be observed that the positions of five modes ( $f_{e1}$ ,  $f_{o1}$ ,  $f_{e2}$ ,  $f_{o2}$  and  $f_{e3}$ ) within the UWB band and the two transmission zeros ( $f_{TZ1}$  and  $f_{TZ2}$ ) are slightly influenced, while  $f_{e4}$  is moved dramatically. After adding the appropriate external coupling by adopting the parallel-coupled lines, the UWB bandwidth is achieved, and a new transmission zero ( $f_{TZ3}$ ) is generated which suppresses  $f_{e4}$  to a certain extent [7]. The length ( $L_3$ ) of the parallel-coupled lines is usually set to be around quarter-wavelength ( $\lambda_g/4$ ) with respect to the UWB filter's central frequency [4].

The dimension  $W_8$  of the cross-shaped stepped-impedance open stubs has an obvious effect on the position of the high mode  $f_{e4}$ . And its initial value can be obtained by analyzing Figure 4(a). Figure 4(a) is the extracted resonator characteristics of the proposed ring resonator with varied  $W_8$ . As  $W_8$  increases from 3.24 to 6.44 mm, there is a slight change in the distribution of the five modes ( $f_{e1}$ ,  $f_{o1}$ ,  $f_{e2}$ ,  $f_{o2}$  and  $f_{e3}$ ) in the passband, and  $f_{TZ3}$  remains approximately constant at 8.05 GHz, while  $f_{e4}$  decreases from 8.25 to 7.81 GHz. When  $W_8$  is set to 4.6 mm, the high mode  $f_{e4}$  can be suppressed by  $f_{TZ3}$ , which can improve the bandwidth of the upper stopband greatly.

Besides, in order to improve the return loss within the passband and obtain sufficient external coupling strength, the proposed ring resonator is fed by a pair of parallel-coupled lines with stepped-impedance ports. As shown in Figure 4(b), the reflection in the passband varies with the parameter  $W_2$  of stepped-impedance ports. It can be seen that when  $W_2$  decreases from 0.816 to 0.116 mm, another transmission pole emerges in the high frequency range.

After the selection of original design values, the proposed UWB filter is optimized by the full-wave electromagnetic simulation software IE3D, and the final associated dimensions of the filter are:  $L_1 = 2.273$ ,  $L_2 = 0.422$ ,  $L_3 = 9.043$ ,  $L_4 = 8.464$ ,  $L_5 = 8.039$ ,  $W_1 = 0.480$ ,  $W_2 = 0.316$ ,  $W_3 = 0.079$ ,  $W_4 = 0.035$ ,  $W_5 = 0.201$ ,  $W_6 = 0.188$ ,  $W_7 = 1.875$ ,  $W_8 = 3.240$ ,  $h_1 = 0.120$ ,  $h_2 = 4.172$ ,  $h_3 = 3.841$ ,  $h_4$

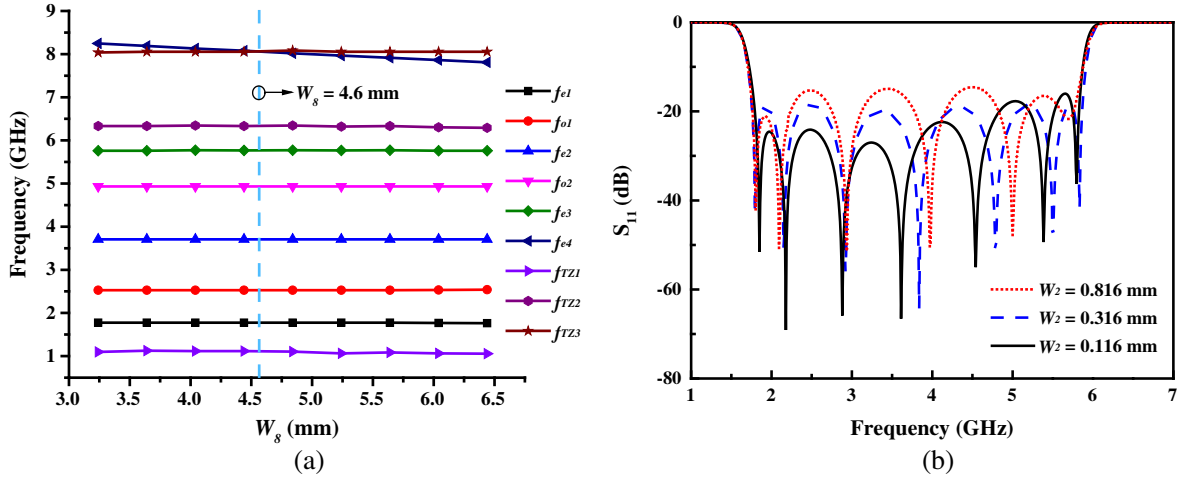
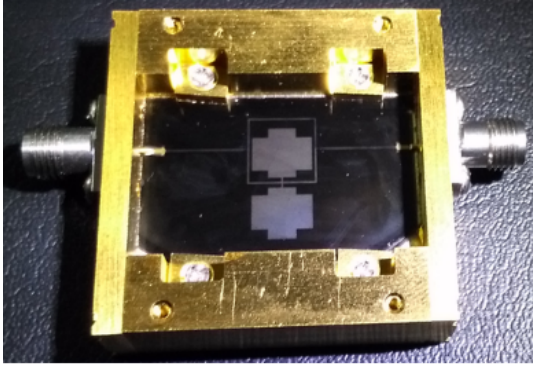
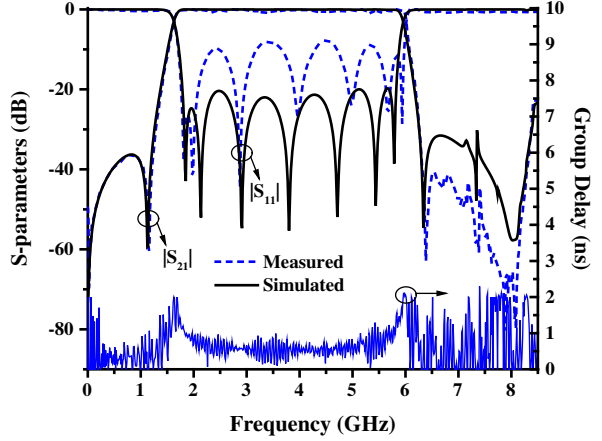


**Figure 4.** Analysis of proposed UWB BPF. (a) Resonator characteristics of the proposed ring resonator with varied  $W_8$ , (b) reflection in the passband with different  $W_2$ .



(a)



(b)

**Figure 5.** Fabricated filter and results. (a) Fabricated HTS UWB filter, (b) simulated and measured results of the HTS UWB filter.

$= 0.505$ ,  $h_5 = 0.879$ ,  $h_6 = 4.038$ ,  $h_7 = 1.146$ ,  $d_1 = 1.017$ ,  $d_2 = 0.438$ ,  $S_1 = 0.034$  (all in millimeter). Then the UWB filter is fabricated on a double-sided YBCO/MgO/YBCO HTS substrate with a size of  $27.63 \text{ mm} \times 14.61 \text{ mm}$  ( $1.11\lambda_g \times 0.58\lambda_g$ ,  $\lambda_g$  is the free space wavelength at center frequency), thickness of 0.5 mm and dielectric constant of 9.8. One side of the HTS films is patterned into the filter circuit by the standard procedure of photolithography and ion etching, and the other side is used for grounding. The filter is then packaged in a metal shield box. A photograph of the HTS UWB filter is shown in Figure 5(a).

The simulated and measured results are shown in Figure 5(b). Owing to the increased resonances from either stepped-impedance ports, the total number of transmission poles is observed to change from 5 to 7 [5]. The measured results show that 3-dB passband covers 1.63 GHz  $\sim$  6.03 GHz. Thanks to the good characteristics of superconducting material, the best insertion loss in the passband is 0.12 dB, and the maximum in-band insertion loss is 0.79 dB. But due to the limited accuracy of fabrication, the return loss is just better than 8.28 dB. The rejection of lower stopband is greater than 36 dB, and the upper stopband with 20 dB attenuation level is extended to at least 8.5 GHz. Besides, the group delay within the UWB passband is between 0.15 and 1.81 ns. Table 1 is the comparison between the proposed UWB BPF with the reported ones.

**Table 1.** Comparison with the reported UWB BPFs.

Ref.	IL (dB)	RL (dB)	S.F. $S.F. = \frac{\Delta f_{3\text{dB}}}{\Delta f_{30\text{dB}}}$	3-dB FBW (%)	Material
[1]	< 1.30	10.6	0.968	111.0	HTS
[2]	< 1.40	11.1	0.902	117.0	Copper
[3]	< 0.80	16.5	0.685	101.9	Copper
[8]	< 0.25	17.5	0.734	108.0	HTS
[9]	< 1.60	12.0	0.920	110.1	Copper
[10]	< 1.00	14.0	0.682	110.0	Copper
This work	< 0.79	8.3	0.885	114.9	HTS

IL: maximum in-band insertion loss; RL: return loss; S.F.: selectivity factor of the passband;  $\Delta f_{3\text{dB}}$ ,  $\Delta f_{30\text{dB}}$ : 3-dB bandwidth and 30-dB bandwidth of the passband, respectively; 3-dB FBW: 3-dB fractional bandwidth of passband.

### 3. CONCLUSION

By constructing a quintuple-mode ring resonator loaded with a pair of symmetrical cross-shaped stepped-impedance open stubs, a UWB BPF with excellent passband selectivity and low insertion loss is successfully designed and fabricated on double-sided YBCO HTS films. And an adverse high mode in upper stopband is effectively suppressed through adjusting the impedance ratio of the cross-shaped stubs and employing a pair of parallel-coupled lines.

### REFERENCES

- Shang, Z. J., X. B. Guo, B. S. Cao, B. Wei, X. P. Zhang, Y. Heng, G. N. Suo, and X. K. Song, "Design of a superconducting ultra-wideband (UWB) bandpass filter with sharp rejection skirts and miniaturized size," *IEEE Microwave Wireless Components Letters*, Vol. 23, No. 2, 72–74, 2013.
- Wu, X. H., Q. X. Chu, X. K. Tian, and X. O. Yang, "Quintuple-mode UWB bandpass filter with sharp roll-off and super-wide upper stopband," *IEEE Microwave Wireless Components Letters*, Vol. 21, No. 12, 661–663, 2011.
- Lan, S. W., M. H. Weng, C. Y. Hung, and S. J. Chang, "Design of a compact ultra-wideband bandpass filter with an extremely broad stopband region," *IEEE Microwave Wireless Components Letters*, Vol. 26, No. 6, 392–394, 2016.
- Zhu, H. and Q. X. Chu, "Ultra-wideband bandpass filter with a notch-band using stub-loaded ring resonator," *IEEE Microwave Wireless Components Letters*, Vol. 23, No. 7, 341–343, 2013.
- Kim, C. H. and K. Chang, "Ultra-wideband (UWB) ring resonator bandpass filter with a notched band," *IEEE Microwave Wireless Components Letters*, Vol. 21, No. 4, 206–208, 2011.
- Moradi, B., U. Martinez-Iranzo, and J. Garcia-Garcia, "Multimode ultra-wideband filters by using a grounded open ring resonator," *Microwave and Optical Technology Letters*, Vol. 58, No. 8, 2001–2004, 2016.
- Kim, C. H. and K. Chang, "Ring resonator bandpass filter with switchable bandwidth using stepped-impedance stubs," *IEEE Transactions on Microwave Theory and Techniques*, Vol. 58, No. 12, 3936–3944, 2010.
- Lu, X. L., B. Wei, Z. Xu, B. S. Cao, X. B. Guo, X. P. Zhang, R. X. Wang, and F. Song, "Superconducting ultra-wideband (UWB) bandpass filter design based on quintuple/quadruple/triple-mode resonator," *IEEE Transactions on Microwave Theory and Techniques*, Vol. 63, No. 4, 1281–1293, 2015.

9. Zhou, C. X., P. P. Guo, K. Zhou, and W. Wu, "Design of a compact uwb filter with high selectivity and superwide stopband," *IEEE Microwave Wireless Components Letters*, Vol. 27, No. 7, 636–638, 2017.
10. Honari, M. M., R. Mirzavand, H. Saghlatoon, and P. Mousavi, "Two-layered substrate integrated waveguide filter for UWB applications," *IEEE Microwave Wireless Components Letters*, Vol. 27, No. 7, 633–635, 2017.